COLLIMATION AND POLARIZATION OF THE JETS IN 3C 219

ALAN H. BRIDLE
National Radio Astronomy Observatory,[a] Edgemont Road, Charlottesville, Virginia 22903-2475

RICHARD A. PERLEY
National Radio Astronomy Observatory, P. O. Box O, Socorro, New Mexico 87801

RICHARD N. HENRIKSEN
Department of Physics, Queen's University at Kingston, Kingston, Ontario K7L 3N6, Canada
Received 18 March 1986; revised 21 May 1986

ABSTRACT

New 4885 MHz VLA maps of the powerful radio galaxy 3C 219 show that the transverse width of its brighter radio jet does not grow significantly between 13 and 35 kpc from its nucleus. An elongated radio knot that is probably part of a counterjet has been discovered. The apparent magnetic field structure of the brighter jet has been mapped at higher resolution than before. The field is well organized, and its mean apparent direction is near the major axis of elongation of the jet over most of the jet's length. Some deviations from this mean direction are systematic, and the largest deviations occur at regular intervals along the jet. The spreading (i.e., lateral expansion) rate of the jet cannot have been constant with distance from the core. If the spreading rate of the synchrotron emission reflects that of an underlying flow, the flow cannot be freely expanding. It is unlikely that the jet is thermally confined by hot gas that is bound to 3C 219 alone, but it may be thermally confined by gas that is bound to the surrounding cluster of galaxies. The radio polarization data neither support nor deny the alternative possibility of magnetically assisted collimation. We suggest further observations to test both alternatives. Some of the asymmetries in brightness and geometry between the main jet and the counterjet in 3C 219 can be accounted for if the jets are symmetric, but contain relativistically moving shocks. Such descriptions of the source are not obligatory, however. In particular, episodic models for the energy transport in 3C 219 can account for some of the source's features, whether or not the jet velocities are relativistic.

I. INTRODUCTION

3C 219 is a luminous ($P = 2.8h^{-2} \times 10^{26}$ W Hz^{-1} at 1.4 GHz, using $H = 100h$ km s^{-1} Mpc^{-1}) radio galaxy with $z = 0.1745$ (Schmidt 1965). It appears to be the dominant member of a cluster of galaxies. Matthews *et al.* (1964) characterize the galaxy as a "cD1: in a D5 envelope, at (the) center of a cluster of richness 2, of which it is by far the brightest member." They also note, from the evidence of a 200 in. plate by Sandage, that "a second fainter galaxy in position angle 120° is joined to the brighter one by a bridge." The radio source has a class II (edge brightened) structure in the Fanaroff and Riley (1974—FR) classification. It contains a prominent jet about $36h^{-1}$ kpc long that was first detected by Turland (1975). Burch (1979), De Young *et al.* (1979), and Högbom (1979) showed that the jet is one-sided and that its apparent magnetic field is aligned with its long axis. Perley *et al.* (1980—PBWF) mapped 3C 219 using 12 antennas of the partially completed NRAO Very Large Array (VLA), showing further that the deconvolved FWHM Φ of the jet does not widen significantly with increasing angular distance Θ from the core.

Many other narrow one-sided jets have since been detected in powerful FR class II sources (e.g., Bridle and Perley 1984). It has also been found that, on the kiloparsec scales accessible to VLA observations in nearby radio galaxies, the *mean* spreading (lateral expansion) rates $d\Phi/d\Theta$ of resolved jets tend to decrease with increasing core and total radio powers (Bridle 1984, 1986). The physical basis of this trend is under debate. Bridle (1986) has summarized evidence that suggests that the internal Mach numbers $\mathcal{M}_j$ of extragalactic jets increase with increasing source power. Furthermore, in the laboratory, the spreading rates of two-dimensional shear layers with $1 \leqslant \mathcal{M} \leqslant 2$ (Bradshaw 1981) and of turbulent round jets in the same range of Mach numbers (Lau 1981) decrease with increasing Mach number $\mathcal{M}$. Bicknell (1986) has argued that the observed relations between spreading rates and radio brightness of extragalactic jets are consistent with the jets in FR class I sources being buoyant turbulent flows with Mach numbers near this critical regime. These phenomenological relationships may therefore provide a framework for understanding the inverse correlation between source power and jet-spreading rates, though the underlying physics needs elaboration. Henriksen (1984b) suggests the alternative that the relation between jet-spreading rate and source power reflects a (turbulently) viscous jet collimation mechanism.

To understand the mechanisms that control jet spreading, we need to know the scales on which $d\Phi/d\Theta$ is determined in extragalactic jets of all powers. In weaker sources (Bridle 1982, 1984, 1986) the jet-spreading rate appears not to be set once and for all on the (presumably subparsec) scale of the "central engine" (e.g., of a black hole accretion disk or its magnetosphere). Instead, jet spreading in such sources appears to be influenced by a mechanism that becomes effective on ~ 10 kpc scales. As 3C 219 provides an opportunity to test whether this is the case in a more powerful source, we reobserved it with the completed VLA at 4885 MHz to obtain higher angular resolution and sensitivity than were available to PBWF.

[a] The National Radio Astronomy Observatory is operated by Associated Universities, Inc., under contract with the National Science Foundation.

 0004-6256/86/030534-12$00.90

II. OBSERVATIONS

We obtained 5 hr of integration on 3C 219 on 8 January 1981 in the VLA "A" configuration (Thompson *et al.* 1980) at 4885 MHz with 50 MHz bandwidth. As the A configuration provides insufficient short baselines to sample the Fourier transform of the extended structure of 3C 219 thoroughly, we added one hour of "C" configuration data on 10 February 1983 to provide the needed short spacings. The flux-density scales of both sets of observations were normalized to that of Baars *et al.* (1977) by observing 3C 286, whose 4885 MHz flux density is 7.41 Jy on this scale. The nearby source 0917 + 449 was used for preliminary phase calibration and to calibrate the instrumental cross-polarization terms. The maps were CLEANed and self-calibrated using the NRAO Astronomical Image Processing System (AIPS), developed by E. W. Greisen, W. D. Cotton, and colleagues.

III. STRUCTURE OF THE CORE AND JETS

a) Total Intensity

Figure 1 shows the distribution of total intensity over 3C 219 at 4885 MHz with 1.″4 ($2.7h^{-1}$ kpc) resolution. The brightest feature in the map is the nuclear core source, whose flux density at 4885 MHz is 51 ± 1 mJy. The jet is the bright narrow feature extending away from the core in position angle ~ − 140°. Its integrated flux density at 4885 MHz is 65 ± 5 mJy. We reserve to a second paper the discussion of the two lobe hot spots and of the more extended emission between and around them, and will concentrate here on the central region of the source.

Figure 2 shows the distribution of total intensity over the central region of the source at 0.″4 ($0.77h^{-1}$ kpc) resolution. At this resolution, the jet comprises two bright segments, linked by a fainter bridge of emission. It contains eight or more internal peaks (knots), many of which appear (at this resolution) to be elongated along the jet's major axis.

The jet emission cannot be traced continuously from the core to the hot spot of the southwest lobe. Figure 2 shows no evidence of jet-like (i.e., narrow) emission in the first 4″ ($8h^{-1}$ kpc) from the core brighter than 100 μJy per CLEAN beam area, or 5% of the peak brightness in the jet (the rms noise on this map is 29 μJy per CLEAN beam area). Figure 1 similarly shows no evidence for narrow emission brighter than 250 μJy per CLEAN beam area in the 50″ ($96h^{-1}$ kpc) between the jet knot furthest from the core and the hot spot in the southwestern lobe. The jet knot furthest from the core ends in a distinct hook or bend (Fig. 2).

The jet is not straight. The position angle of its ridge line changes from − 136° in the first 10″ to − 147° in the last 5″; much of this 11° deflection apparently occurs within the fainter bridge of emission that links the jet's two brightest

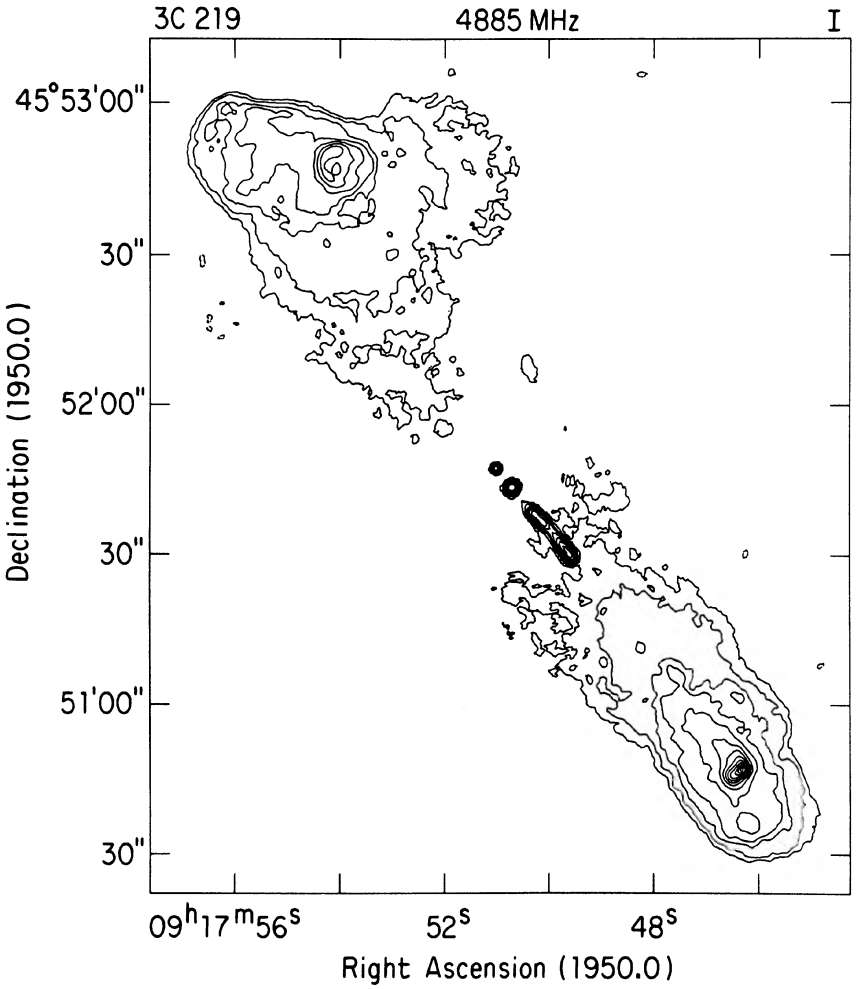

FIG. 1. Total intensity distribution across 3C 219 at 4885 MHz, CLEANed and restored with a Gaussian beam of FWHM 1.″4. Contours are drawn at − 1, 1, 2, 4, 6, 10, 16, 24, 34, 46, 60, 76, 90, and 106 times 0.25 mJy per CLEAN beam area. The extended emission ~20″ to the north of the core and the jet is part of an extended confusing source that will be discussed in a second paper.

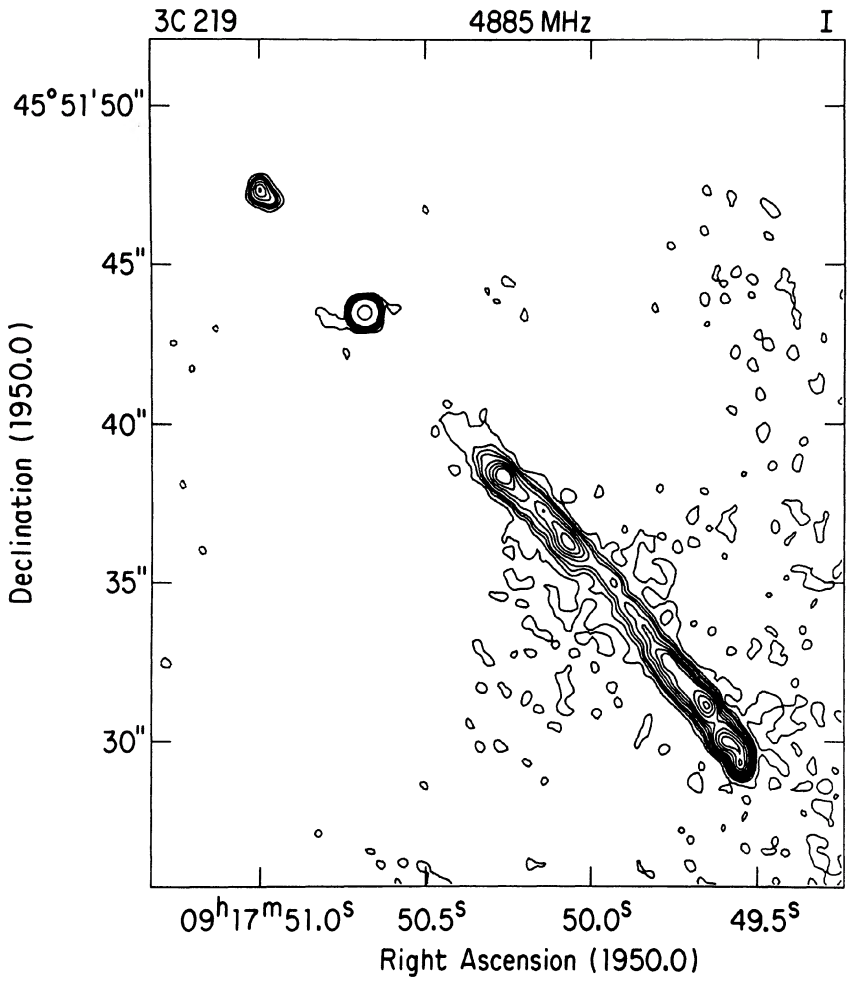

FIG. 2. Total intensity distribution over the central region of 3C 219 at 4885 MHz, CLEANed and restored with a Gaussian beam of FWHM 0".4. Contours are drawn at − 1, 1, 2, 3, 4, 6, 8, 10, 12, 16, 20, 24, and 214.5 times 0.1 mJy per CLEAN beam area. The circular contour around the peak of the core source shows the FWHM of the restoring beam.

segments. The ridge line defined by the inner pair of knots also passes about 1" south of the core, suggesting a further misalignment between the jet and the core.

Figures 1 and 2 both show a discrete elongated knot ~5" ($9.6h^{-1}$ kpc) from the core on the jet axis but to the northeast of the core. This knot has an integrated flux density of 2.3 mJy at 4885 MHz and was blended with more diffuse structure on the less sensitive maps of 3C 219 hitherto available. Sky surveys at 4755 MHz (Ledden *et al.* 1980) show that the mean density of sources stronger than 2.3 mJy at this frequency at high galactic latitudes is only 0.012 per square arcmin. The knot is therefore most unlikely to be a random confusing source. As the knot lies on the continuation of the jet axis through the core toward the northeast, and is itself elongated along position angle − 136°, it is likely that it is the brightest feature of a counterjet in 3C 219. We therefore describe it as such below. The lobeward edge of this knot has a sharper brightness gradient than does the coreward edge (Fig. 2).

b) Polarized Intensity

The core is $\leqslant 0.2\%$ linearly polarized at 4885 MHz; the only polarized signal measured at this position is consistent with instrumental residuals.

Figure 3 shows the observed distribution of the 4885 MHz *E* vector intensities and orientations over the main jet at 0".4 resolution, superposed on the second total intensity contour from Fig. 2. The polarized intensity distribution has been corrected for the Ricean bias (the rms noise on the maps of Stokes *Q* and *U* is 29 μJy per CLEAN beam area, identical to that in Fig. 2). The shortest vector shown corresponds to a polarized intensity of 90 μJy per CLEAN beam area.

Figure 4 shows a gray-scale display of the distribution over the main jet of the percentage of linear polarization ($100\sqrt{Q^2+U^2}/I$), again superposed on the second intensity contour from Fig. 2. The percentage of polarization varies from $<10\%$ near the southwest tip of the jet to 58% ($\pm 6\%$) along its western edge. The percentage of polarization is generally higher on the western edge of the jet than on the eastern edge. The percentage of polarization is also generally higher in the fainter emission than in the brighter—i.e., the polarized intensity is more constant along the jet than is the total intensity, a phenomenon previously documented in the jet of NGC 315 by Willis *et al.* (1981). Note that the polarized intensity at the extreme southwestern tip of the jet falls below the 3σ cutoff level adopted for Figs. 3 and 4. There is evidence from Fig. 3 that the *E* vector orientations at this end of the jet change significantly on the scale of our beam. This "depolarization" at the end of the jet may therefore be at least partially an artifact of finite resolution.

The peak linearly polarized intensity of the counterjet knot at 0".4 resolution is 0.14 mJy in position angle 72°; the

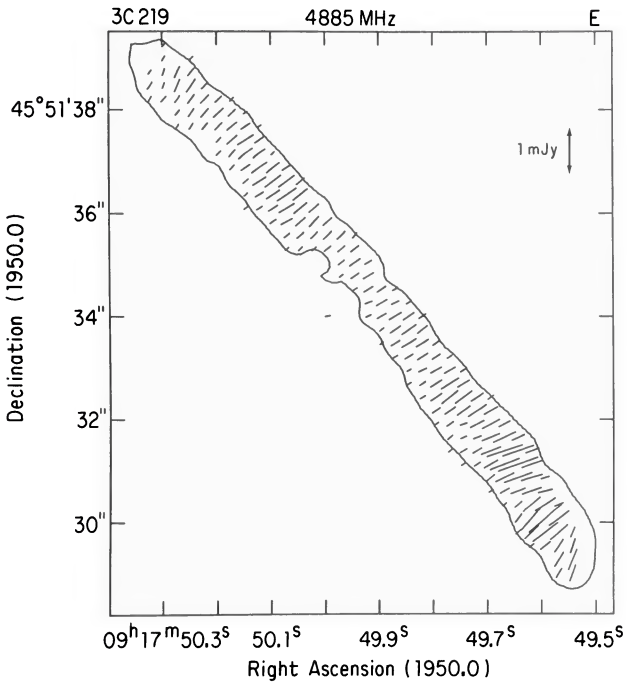

FIG. 3. Distribution of 4885 MHz E vector intensities and position angles over the jet in 3C 219 at 0".4 resolution, superposed on the 0.2 mJy per CLEAN beam area contour from Fig. 2. No vectors below 90 μJy per CLEAN beam area (3σ) are plotted. The vectors are plotted at intervals of 0".26, so adjacent vectors are partially correlated by the synthesized beam.

percentage of polarization there is $\approx 14\%$. This peak occurs near the outer edge of the knot. Over most of the knot, the linearly polarized intensity is too small to be measured reliably at this resolution.

c) The Magnetic Field Direction in the Jet

We have compared VLA maps (not shown here) of 3C 219 at 3" resolution at 1465 and 4885 MHz, and find that the Faraday rotation measure of the jet ranges from about -5 to -15 rad m^{-2} along its length, provided there is no 180° ambiguity in the apparent E vector position angles. The absence of a 180° ambiguity is supported by the 2695 and 8085 MHz data of Burch (1979) and De Young *et al.* (1979). The integrated rotation measure derived for 3C 219 by Simard-Normandin *et al.* (1981) is -19 ± 2 rad m^{-2}, consistent with this supposition.

The E vector orientations shown in Fig. 3 at 0".4 resolution should therefore be within $\leqslant 3°$ of their "intrinsic", i.e., infinite-frequency, values everywhere along the jet. Figure 5 shows the derived directions of the "apparent" (i.e., synchrotron emissivity weighted and vector averaged) magnetic field $\mathbf{B}_a$, plotted as vectors with lengths showing the percentage of linear polarization at 4885 MHz and orientations showing the inferred magnetic field direction. Note that both the lengths and the relative orientations of these vectors measure the degree of orderliness of the field in directions perpendicular to the line of sight.

Even though the beam area in these data is over six times smaller than that of the 4885 MHz observations by PBWF, the apparent magnetic field $\mathbf{B}_a$ still appears to be well ordered and approximately parallel to the jet's long axis. The mean value of the magnetic field position angles depicted in Fig. 5 is $-142°$, with an rms dispersion of 12°. This mean value is close to the mean position angle of the jet (Sec. III*a*). Part of the observed variance in the orientation of $\mathbf{B}_a$ arises from changes in direction of the magnetic field as it follows the local ridge line of the jet. Figure 5 clearly shows some locally systematic deviations of up to 25° from the mean field orientation, however, especially toward the lobeward end of

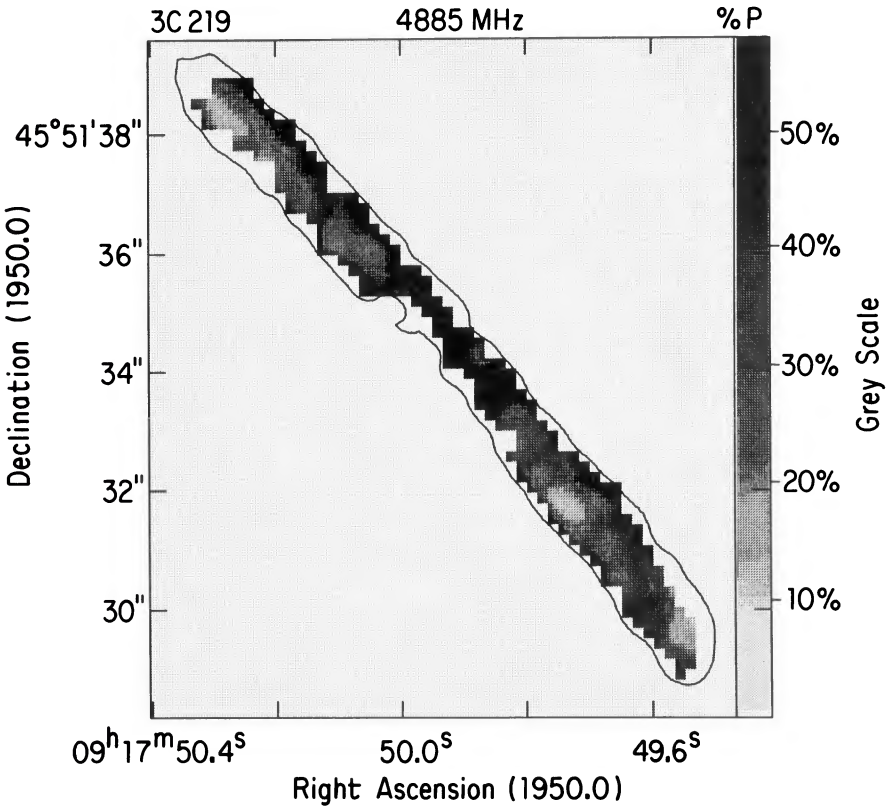

FIG. 4. Gray-scale display of the distribution of the percentage of linear polarization at 4885 MHz over the jet in 3C 219, for positions where the polarized intensity exceeds 90 μJy per CLEAN beam area.

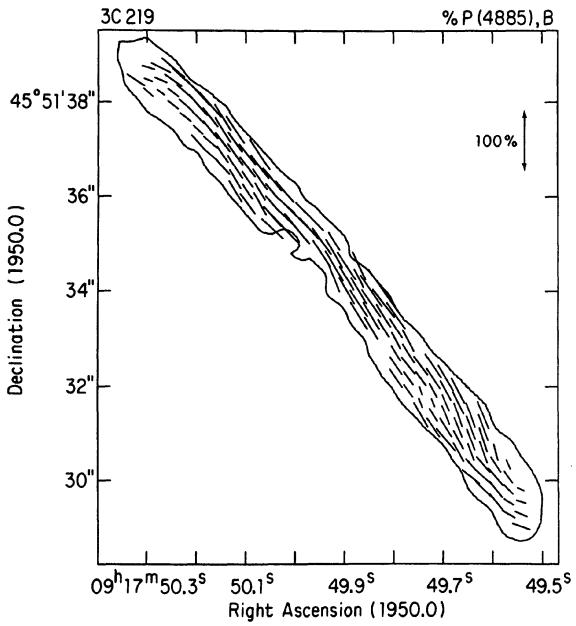

FIG. 5. Inferred distribution of apparent magnetic field orientation over the jet in 3C 219. The vector lengths are proportional to the percentage of linear polarization at 4885 MHz; their orientations are at right angles to those of E vectors in Fig. 3.

the jet. The regions where the apparent field direction deviates most significantly from the jet axis occur at intervals of $\approx 3''.5$ along the jet.

The orientation of $\mathbf{B}_a$ at the counterjet knot also deviates significantly from the mean direction. At the peak of the polarized intensity in this knot, the apparent field direction is in position angle $-18°$, or 56° from the mean field direction along the main jet.

IV. THE COLLIMATION DATA

To determine how the jet FWHM Φ changes with angular distance Θ from the core, we made a further map from which the data on baselines $< 40\ k\lambda$ long were excluded. This exclusion has two effects. First, the resolution of the synthesized beam is slightly improved, to $0''.35$ ($0.67h^{-1}$ kpc). Second, excluding the shorter baselines filters out the low-level "rumble" due to weak extended emission in the region around the jet (see Fig. 2). This flattens the baselines against which we measure the widths of the transverse intensity profiles across the jet. We fitted these profiles with Gaussian functions, as the profiles were all described well by this form.

Deconvolving the instrumental beam from the fitted Gaussian FWHM and peak intensity data in the usual way (e.g., Perley *et al.* 1984; Killeen *et al.* 1986), we found the jet parameters listed in Table I. The deconvolved FWHM Φ of the jet does not increase systematically in the regime $6''.6 \leqslant \Theta \leqslant 18''$ ($13h^{-1}$ to $35h^{-1}$ kpc) from the core (see Fig. 6).

While this confirms the qualitative result deduced by PBWF, our new measures of Φ are smaller (at some distances from the core, significantly smaller) than those of PBWF. We attribute this to the poorer signal-to-noise and lower resolution across the jet in the PBWF data, especially closest to the core [compare our Fig. 2 with Fig. 2(b) of PBWF]. We believe that this discrepancy is mainly a signal-to-noise effect, as our own data at $1''.4$ resolution give estimates of, or upper limits to, Φ that agree well with our results at $0''.35$ resolution. Figure 2(b) of PBWF also suggests that blending of the jet with more diffuse emission may have led PBWF to overestimate the jet width in some of its fainter regions.

The data for the main jet in Fig. 6 (dark circles) imply that the jet widens rapidly within $6''.6$ ($13h^{-1}$ kpc) of the core, but spreads more slowly, if at all, further out. The FWHM of the counterjet knot (plotted in Fig. 6 as a light circle, folded over the same side as the main jet data) also suggests a rapid spreading in the first $\leqslant 10h^{-1}$ kpc. Our data clearly do not support the notion that the radio jet spreads at a constant rate from a negligible width close to the core.

We therefore conclude that, *if the synchrotron spreading rate reflects that of the underlying flow in 3C 219*, the collimation properties of this flow were not set once and for all by initial conditions at the central engine. Instead, some mechanism that took effect on scales $\leqslant 10h^{-1}$ kpc from the core slowed the mean spreading rate of the jet relative to that achieved closer to the core. We cannot determine exactly where this recollimation took effect, but we argue below that the brightening of the radio jet may be closely related to the recollimation process. If this is correct, recollimation probably occurred on a scale of order $5h^{-1}$ kpc to $10h^{-1}$ kpc from the core.

TABLE I. Collimation and physical parameters of jets in 3C 219.

Angular distance from core Θ (arcsec)	Deconvolved FWHM Φ (arcsec)	Deconvolved peak intensity I (mJy)	Equipartition field strength B_{eq} (Gauss)	Minimum pressure nT (cm^{-3} K)
Main Jet				
6.60	0.54 ± 0.05	1.42 ± 0.03	$6.7h^{2/7} \times 10^{-5}$	$8.8h^{4/7} \times 10^{5}$
7.50	0.72 ± 0.07	0.59 ± 0.02	$4.9h^{2/7} \times 10^{-5}$	$4.7h^{4/7} \times 10^{5}$
9.76	0.56 ± 0.07	1.17 ± 0.05	$6.2h^{2/7} \times 10^{-5}$	$7.5h^{4/7} \times 10^{5}$
12.88	0.41 ± 0.06	0.51 ± 0.02	$5.3h^{2/7} \times 10^{-5}$	$5.4h^{4/7} \times 10^{5}$
14.7	0.58 ± 0.06	1.32 ± 0.06	$6.5h^{2/7} \times 10^{-5}$	$8.2h^{4/7} \times 10^{5}$
15.4	0.51 ± 0.10	1.17 ± 0.04	$5.9h^{2/7} \times 10^{-5}$	$6.8h^{4/7} \times 10^{5}$
16.32	0.46 ± 0.04	2.51 ± 0.08	$8.2h^{2/7} \times 10^{-5}$	$1.3h^{4/7} \times 10^{6}$
17.16	0.70 ± 0.08	1.06 ± 0.03	$5.9h^{2/7} \times 10^{-5}$	$6.6h^{4/7} \times 10^{5}$
18.14	0.51 ± 0.05	2.46 ± 0.07	$8.0h^{2/7} \times 10^{-5}$	$1.2h^{4/7} \times 10^{6}$
Counterjet				
-5.08	0.40 ± 0.03	1.22 ± 0.04	$6.8h^{2/7} \times 10^{-5}$	$9.0h^{4/7} \times 10^{5}$

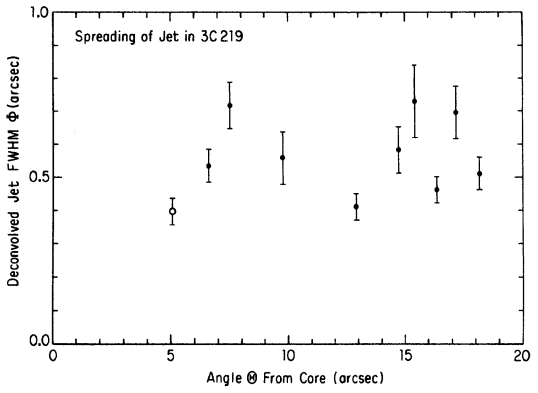

FIG. 6. Plot of the deconvolved FWHM Φ of the jet's transverse brightness profile against angular distance Θ from the core, to show the spreading of the synchrotron emission. 1σ error bars are shown at each point. The dark circles are data from profiles taken across the main jet. The light circle is from a profile taken across the peak of the counterjet knot.

V. CAN THE JETS BE THERMALLY CONFINED?

The collimation behavior described in Sec. IV resembles that of the jets in several weaker radio galaxies (e.g., NGC 315—Willis *et al.* 1981, Bridle 1982; 3C 31—Bridle *et al.* 1980; B2 1321 + 31—Fanti *et al.* 1982; NGC 6251—Perley *et al.* 1984; IC 4296—Killeen *et al.* 1986) in that there is evidence for initially rapid jet spreading followed by slower spreading once the jet has traveled from $1h^{-1}$ to $10h^{-1}$ kpc from the core. The minimum pressures $p_{\rm min}$ of the relativistic particles and magnetic fields in the kiloparsec-scale jets of these weaker radio galaxies can be confined by the external gas pressure $p_{\rm ext} = nkT$ in the hot gaseous halos of these galaxies without implying thermal bremsstrahlung luminosities that conflict with the available *Einstein* Observatory x-ray data. We now consider whether the jet in 3C 219 might also be recollimated by the thermal pressure of hot gas surrounding the radio source.

We have estimated the minimum pressure $p_{\rm min}$ of the relativistic electrons and magnetic fields in the jet and counterjet of 3C 219 using the following assumptions. We assume that the spectrum of the jets is a $\nu^{-0.8}$ law from 10 MHz to 100 GHz (the observed spectra along the jet between 1465 and 4885 MHz at 1".4 resolution range from $\nu^{-0.62}$ to $\nu^{-0.96}$, most of this variance being due to noise in fainter regions of the jet). We also assume that the jets are filled regions whose depth in the plane of the sky is equal to their transverse deconvolved FWHM, and that equal energies reside in relativistic particles of each charge. With these assumptions, the range of $p_{\rm min}$ along the jet and the counterjet at the locations at which transverse FWHMs were measured corresponds to $4.5h^{4/7}\times 10^5$ cm^{-3} K $\leqslant nT \leqslant 1.3h^{4/7}\times 10^6$ cm^{-3} K (Table I).

These minimum pressures do not decrease systematically with distance from the core. This fact, their 3:1 range of values, and the limited range of distances from the core at which the jet has been detected complicate any assessment of whether the jet and counterjet in 3C 219 could be recollimated (after an initial rapid spreading) by the thermal pressure of an external medium. This assessment is easier for the jets in the weaker radio galaxies referred to above—in these sources the jets can be traced over a wider range of $p_{\rm min}$, so the form of $p_{\rm ext}$ required to confine them is much clearer. Nevertheless, we may draw some broad conclusions for 3C 219.

First, we note that *if* the main jet is recollimated by the external pressure $\sim 5h^{-1}$ to $10h^{-1}$ kpc from the core, then its total pressure $p_{\rm j}$ should be $\approx p_{\rm ext}$ at these distances from the core, but the recollimation process would be expected to produce an internal shock cell pattern downstream from the recollimation region (e.g., Sanders 1983). If this has occurred in 3C 219, the brighter radio knots in the jet might be the result of relativistic particle reacceleration and compression of the jet fluid by such shocks; i.e., the recollimation process may be intimately related to the sudden brightening of the jet that permits us to observe it.

Segments of a jet that have been shocked in this way could be overpressured relative to the surrounding medium by factors up to $\mathcal{M}_{\rm j}^2$, but, lacking an independent estimate of $\mathcal{M}_{\rm j}$ for this jet, we cannot estimate how large the resulting overpressures might be in 3C 219. We will, however, assume that only the *fainter* parts of the synchrotron jet need be in pressure balance with the external medium for the flow as a whole to have been recollimated. Making the conventional assumption that the total jet pressure $p_{\rm j}$ is about equal to $p_{\rm min}$, we therefore interpret Table I to mean that $p_{\rm ext} \approx 6.5h^{4/7}\times 10^5$ cm^{-3} K at $35h^{-1}$ kpc from the core (near the lobeward end of the jet). As the variation in the external pressure along the jet is also unlikely to exceed the range of pressures *within* the jet, we also require that $p_{\rm ext} \leqslant 1.3h^{4/7}\times 10^6$ cm^{-3} K (the highest value "observed" in the jet) where the jet first brightens ($10h^{-1}$ kpc from the core).

To examine the range of parameters within which the jet might be thermally confined, we must model the putative confining atmosphere. We adopt, for illustrative purposes, the hydrostatic isothermal model that is commonly used to interpret x-ray observations of gaseous halos of galaxies and galaxy clusters (e.g., Cavaliere and Fusco-Femiano 1976; Jones and Forman 1984). That is, we take the atmosphere to be gravitationally bound to stellar matter (the 3C 219 galaxy or cluster) whose density $\rho(r)$ as a function of distance r from the center of 3C 219 is given roughly by the King approximation $\rho(r) = \rho(0)\times(1 + (r^2/r_{\rm c}^2))^{-3/2}$. The hydrostatic isothermal number density distribution of the gas then obeys $n(r) = n(0)\times(1 + (r^2/r_{\rm c}^2))^{-3\beta/2}$, where $\beta = \mu m_{\rm p}\sigma_{\rm r}^2/kT$. Here μ is the mean molecular weight of the gas, $\sigma_{\rm r}$ is the radial velocity dispersion of the stellar matter, and T is the gas temperature (all taken to be constant in this approximation).

Estimates of β from observations of the brightness distribution of 0.5–3 keV x-ray emission around single elliptical galaxies range from 0.45 to 0.6 (Forman *et al.* 1985) and in clusters of galaxies range from 0.4 to 1, with a mean near $\beta = 2/3$ (Jones and Forman 1984; Henriksen and Mushotzky 1985). Estimates of β in clusters from observed radial-velocity dispersions and x-ray temperatures lead to higher values, with a mean near $\beta = 1.2$ (Mushotzky 1985). This discrepancy and the lack of correlation between the core radii $r_{\rm c}$ derived from x-ray and from optical cluster data give reason for concern about the consistency of the approximations made in the standard hydrostatic isothermal models (e.g., Henriksen and Mushotzky 1985). Nevertheless, such models are probably adequate for our purpose, which is merely to determine the order of magnitude of the temperature, density, and linear-scale parameters required to confine this jet thermally. We have made calculations with

$\beta = 2/3$ and $\beta = 1$ to assess how our conclusions depend on β.

We apply the available constraints as follows. Our constraint on $p_{ext}(r)$ at $10h^{-1} \leqslant r \leqslant 35h^{-1}$ kpc determines a *minimum* value of the core radius r_c, assuming that the nucleus of 3C 219 is at $r = 0$. If r_c is too small, p_{ext} falls too rapidly with r to fit the jet pressures inferred above. For any assumed value of the gas temperature T, we then compute a lower limit (corresponding to the lower limits for p_j and for r_c) to the central electron density $n_e(0)$ required to confine the jet. From this and r_c we compute a lower limit to the total x-ray bremsstrahlung luminosity L_x that would be expected from 3C 219 between 0.5 and 3 keV if the jet is confined by gas with the assumed temperature T. The value of L_x is constrained by the *Einstein* Observatory IPC data for 3C 219; Fabbiano *et al.* (1984) observed $L_x = 6h^{-2} \times 10^{43}$ erg s^{-1} between 0.5 and 3 keV in the direction of 3C 219. The value of L_x obtained by integrating over the model atmosphere must not exceed this. Indeed, the correlation observed by these authors between total x-ray powers and radio core powers of radio galaxies suggests that some of the x-ray emission from radio galaxies originates in their nuclei. The constraint on the value of L_x from 10 kpc scale hot gas associated with 3C 219 might therefore be tightened if the nuclear x-ray contribution could be separately measured and subtracted from the total.

For a given assumed gas temperature T, there is also a *maximum* value of r_c which can fit the pressure at the end of the jet without exceeding the observed value of L_x (the predicted x-ray luminosity varies as r_c^3). This maximum value of r_c decreases with T, and below some minimum temperature it conflicts with the minimum value of r_c set by the variation of p_j. At temperatures below this minimum, the available constraints cannot be reconciled with thermal confinement for *any* combination of r_c, T, and $n(0)$.

For $\beta = 1$, the minimum value of r_c that is consistent with thermal confinement of the jet is $43h^{-1}$ kpc, and the minimum value of T is 3.6×10^7 K. For $\beta = 2/3$, thermal confinement is possible only if $r_c \geqslant 33h^{-1}$ kpc and $T \geqslant 4.8 \times 10^7$ K. For either value of β, the minimum values of r_c and T that are required to confine the jet thermally exceed those observed in the x-ray halos of any single elliptical galaxy (Forman *et al.* 1985), though the temperature in the M87 halo on the relevant scale is $\sim 3 \times 10^7$ K (Fabricant *et al.* 1980; Lea *et al.* 1982), approaching the minimum temperature required for thermal confinement if $\beta \approx 1$.

As our estimates of p_j and p_{ext} are lower limits, and thermal confinement of even the *faintest* detected parts of the jet implies more than the total observed luminosity between 0.5 and 3 keV if the gas temperature is $\leqslant 3.6 \times 10^7$ K, we conclude that the 3C 219 jet is most unlikely to be recollimated by gas that is bound to the parent galaxy alone. Note that this conclusion is virtually independent of the value of h, as the observed value of L_x scales as h^{-2}, while the value required for thermal confinement scales as $h^{-13/7}$.

We cannot, however, exclude the possibility that the jet is recollimated by gas that is bound to the 3C 219 cluster as a whole. The survey of x-ray properties of clusters by Jones and Forman (1984) contains many examples of clusters with gas temperatures $> 4.6 \times 10^7$ K, and it contains some with temperatures $> 10^8$ K. The x-ray luminosity that is observed at 3C 219 is also not unusually high for a cluster atmosphere. Even with the more restrictive choice of $\beta = 2/3$, thermal confinement of the 3C 219 jet by an intracluster atmosphere is possible within the range of cluster x-ray parameters found by Jones and Forman. For example, with $\beta = 2/3$ and a temperature of 7×10^7 K (corresponding to a cluster with a radial-velocity dispersion $\sigma_r = 780$ km s^{-1}) the constraints can be satisfied with core radii in the range $33h^{-1} \leqslant r_c \leqslant 59h^{-1}$ kpc, and central densities in the range $2h^{4/7} \times 10^{-2} \geqslant n(0) \geqslant 1.3h^{4/7} \times 10^{-2}$ cm^{-3}. These parameters correspond to radiative cooling times t_c from $3.6h^{-4/7}$ to $5.6h^{-4/7} \times 10^9$ years in the cluster center. Alternatively, at $T = 10^8$ K, on the upper edge of observed cluster gas temperatures (corresponding to a radial-velocity dispersion of 940 km s^{-1}) thermal confinement would be possible within the constraints for $33h^{-1} \leqslant r_c \leqslant 85h^{-1}$ kpc, $1.4h^{4/7} \times 10^{-2} \geqslant n(0) \geqslant 7.7h^{4/7} \times 10^{-3}$ cm^{-3}, and cooling times $6.1h^{-4/7} \times 10^9 \leqslant t_c \leqslant 1.1h^{-4/7} \times 10^{10}$ yr.

These values of $n(0)$, T, and r_c resemble those of "evolved XD" clusters in the language of Jones and Forman (1984); these are clusters with central, dominant galaxies, high x-ray luminosities, and high central galaxy densities.

To summarize, it is unlikely that the jets in 3C 219 can be confined by hot gas that is bound to 3C 219 alone, but they might be confined by hot gas that is bound to the surrounding cluster, if such gas has parameters similar to those found in evolved XD clusters such as Abell 85, Abell 1795, and Perseus. The radio jet might indeed "light up" at ~ 10 kpc from the nucleus of 3C 219 owing to changes in its internal structure (e.g., shocks) that are induced by encountering the slowly declining pressure in the cluster atmosphere after previously propagating (freely?) down a steeper pressure gradient in the galaxy atmosphere. The following data will help to test whether the jets are indeed recollimated by the pressure of gas that is bound to the cluster as a whole:

(a) improved images of the x-ray emission for about 10″–30″ around the 3C 219 galaxy at keV energies,
(b) estimates of the temperature of extended x-ray emission around 3C 219,
(c) measurements of the radial velocities of the fainter galaxies around 3C 219, to check that the cluster is indeed associated with the radio galaxy and to determine its velocity dispersion,
(d) indications of a cooling flow in the cluster, such as low-ionization x-ray line emission or optical emission-line filaments, close to 3C 219 (as the cooling time implied by thermal confinement may be short, especially at the lower temperatures). Absence of such features would not rule out thermal confinement, however, if the cluster contains significant heat sources for the gas (e.g., Miller 1986).

VI. CAN THE JETS BE MAGNETICALLY CONFINED?

If future x-ray observations rule out thermal confinement for this jet, our data will require either that another confinement mechanism be found or that we consider models in which the spreading rate of the synchrotron-emitting particles or the magnetic fields, or both, can be less than that of the underlying flow.

Magnetically assisted confinement is often discussed as a possible nonthermal collimation mechanism for extragalactic radio jets. In this mechanism, the $\mathbf{J} \times \mathbf{B}$ forces between azimuthal field loops and a current carried by the jet (e.g., Benford 1979, 1983; Bicknell and Henriksen 1980; Chan and Henriksen 1980; Bridle *et al.* 1981; Rees 1982; Begelman *et*

al. 1984) are invoked to mediate between a high pressure near the axis of a jet and a lower external, e.g., thermal, pressure far from the axis. A predominantly azimuthal **B** field must wrap the jet for this mechanism to be effective.

Figure 5 clearly shows that the *apparent* magnetic field $\mathbf{B}_a$ in the synchrotron jet of 3C 219 is parallel to the jet over most of its length. We emphasize that there are at least two ways in which this apparent field configuration might be compatible with that required for magnetically assisted collimation:

(1) The jet may be too poorly resolved (Bridle 1982). Because there are only about two synthesized beam widths across the FWHM of the jet at most distances from the core, the observed apparent field distribution significantly blends information from the edges of the jet and from its center. For many different helical field configurations, the synchrotron radiation from particles with an isotropic pitch angle distribution appears most highly polarized near the edges of the jet, where $\mathbf{B}_a$ is parallel to the jet axis for a wide range of orientations of the jet relative to the observer (e.g., Laing 1981b, Figs. 2 and 3). Unless the jet axis is near the plane of the sky, only a strip near the center of the jet exhibits $\mathbf{B}_a$ perpendicular to the jet axis. There is a wide range of jet orientations (for any given field configuration) within which this $\mathbf{B}_a$-perpendicular band would be weakly polarized relative to one or both edges of the jet. The "perpendicular-field" signature of a helical configuration field might therefore be "blended out" (as a region of reduced polarization) at low transverse resolution. The jet in 3C 219 might therefore have a magnetic field with substantial azimuthal component if its axis is not near the plane of the sky.

(2) The confining azimuthal field may lie *outside* the bright synchrotron-emitting jet, in the weak extended emission that surrounds it (Begelman *et al.* 1984). If the organized component of the field in the jet has a configuration resembling the Chan-Henriksen (1980) "flux rope" (in which the ratio B_ϕ/B_z increases radially outward from the jet axis), the balance between apparently parallel and perpendicular components of $\mathbf{B}_a$ in the synchrotron emission from a jet is extremely sensitive to the radial distribution of the relativistic electrons. Concentration of these particles toward the axis of the jet could suppress the signature of any outer azimuthal field regions in the overall polarization distribution.

Alternative (1) may best be tested by higher-resolution polarimetry of the jet itself, e.g., by using the VLA at frequencies above 4885 MHz. Transverse profiles of the percentage of linear polarization, of $\mathbf{B}_a$, and of the total intensity across the jet at higher resolution could be compared with the predictions of different jet models (e.g., as in Perley *et al.* 1984) to set limits to the azimuthal field contribution in the bright synchrotron-emitting region.

In this context, it is interesting that the model of force-free equilibrium of a thermally confined but magnetic pressure-dominated jet by Königl and Choudhuri (1985—KC) predicts several features that agree qualitatively, but not quantitatively, with our observations of 3C 219. Their model predicts, among other things, (a) that regions where $\mathbf{B}_a$ is oblique to the jet axis will occur at periodic intervals along such a jet once it has traveled sufficiently far from its source, (b) that the total intensity ridge line will oscillate in direction with the same wavelength as the apparent field oscillations, and (c) that the percentage of linear polarization and the total intensity will vary in antiphase with each other, and with half this wavelength. The jet in 3C 219 indeed exhibits oblique field regions, ridge-line deflections, and inversely correlated variations in the percentage of polarization and the total intensity (Figs. 5, 2, and 4, respectively). There are also about two intensity knots per cycle of the field orientation along the jet, as expected on the KC model. At the resolution of our data, however, these phenomena appear to have wavelengths longer than those predicted by the KC model. The separation of the oblique field regions along the jet according to the model should be $5R\cos\iota$, where R is the jet radius and ι is the angle between the jet axis and the plane of the sky. If we identify the jet radius R with $\Phi/2$, then the observed separation of the oblique-field regions in 3C 219 is $\approx 10R$, about twice the maximum expected on the model. It is conceivable, however, that fluctuations of smaller amplitude and wavelength would escape detection with our limited resolution transverse to the jet, so this wavelength discrepancy should be re-examined at higher resolution.

We stress the need to test the predictions of such magnetized-jet models quantitatively, as each of the predicted features could separately be caused by other phenomena. For example, the inverse correlation between percentage of polarization and intensity is expected in any model that appeals to particle acceleration by turbulence.

Alternative (2) may be tested by sensitive high-resolution polarimetry of the region around the jet at *low* frequencies. Burch (1979) mapped the distribution of $\mathbf{B}_a$ in the lobe around the jet in 3C 219. His Fig. 10 shows a region where $\mathbf{B}_a$ is perpendicular to the jet, outside it and to the southeast. It would, however, be quite incorrect to regard this observation, as it stands, as a hint of the azimuthal field required for magnetically assisted confinement. There are two main reasons for this.

First, the field observed by Burch in this region is part of a larger-scale distribution of $\mathbf{B}_a$ and of the percentage of linear polarization over the southwest lobe of 3C 219 that resembles the tangled field model "C" of Laing (1981b, his Fig. 6a) for a source about 30° from the line of sight. Laing's field model contains a distribution of tangled field loops that would not confine the jet. The presence of perpendicular $\mathbf{B}_a$ in the more extended emission near the jet does not *by itself* provide evidence for magnetically assisted collimation of the jet, any more than the apparently parallel field along the jet provides evidence against such collimation.

Second, there is only a restricted range of circumstances within which synchrotron radiation from a helically wound field produces $\mathbf{B}_a$ perpendicular to the jet axis at its *edges* (Laing 1981b). These circumstances require (a) that the helix be tightly wound into the azimuthal plane ($B_\phi \gg B_z$) *and* (b) that the jet axis be near the plane of the sky. It is statistically more plausible that the field documented by Burch is part of a tangled configuration of the sort described by Laing than that it is part of a large-scale helix wrapping the jet.

The Laing field might, however, be distinguished from a jet-confining configuration by studying the Faraday rotation gradient in the lobe near the jet. The Laing field would not produce an organized rotation measure gradient across the jet. In contrast, the reversal of the sign of $\int B_\parallel dl$ across a wrapped-loop configuration will produce a rotation measure gradient across the jet at sufficiently low frequencies, unless the jet lies close to the line of sight, so that the field loops are near the plane of the sky. It may therefore be possible to distinguish observationally between the Laing fields and the

wrapped-loop configurations—if there is enough thermal material around the jet to render the azimuthal-field region Faraday thick at frequencies between 0.3 and 3 GHz (where ionospheric effects and synthesis-array dimensions and sensitivities permit radio polarimetry at arcsecond resolution). High resolution would be essential for this test, as the Faraday rotation expected across an azimuthal field goes to zero both near the center of the jet (where $B_{\|} \rightarrow 0$) and at its edges (where $\int dl \rightarrow 0$).

VII. THE JET/COUNTERJET ASYMMETRIES

Can the jet/counterjet asymmetries in 3C 219 be ascribed to Doppler favoritism of the approaching side of a symmetric flow with velocity $v_j \approx c$ (e.g., Blandford and Königl 1979a)? We will consider several types of relativistic jet models.

a) Smooth, Symmetric Relativistic Flows

The simplest relativistic jet model is that in which the only asymmetries seen by an observer are produced by the Doppler effect in a steady, smooth symmetric outflow with a unique velocity $v_j = \beta_j c$. In this model, the counterjet would be a faint replica of a smooth main jet. The brightness ratio between the two jets would be given by the constant factor

$$\left(\frac{1+\beta_j \sin \iota}{1-\beta_j \sin \iota}\right)^{(2+\alpha)}, \tag{1}$$

where α is the radio spectral index and ι is the angle between $\mathbf{v}_j$ and the plane of the sky.

This model is too simple to account for the observed features of 3C 219—the counterjet is not simply a faint replica of the main jet, and both jets contain knots. The model is also physically naive. Jets are unlikely to be steady, smooth, or of uniform velocity. In particular, many different processes can produce shocks in real jets (e.g., Smarr *et al.* 1984). These processes include interactions between the outflowing material and the surrounding medium, and time variations in the properties of the outflow.

b) Symmetric Relativistic Flows with Stationary Shocks

Whether or not relativistic seed particles are actually reaccelerated at shocks, compression of the flow near a shock will enhance the synchrotron emissivity by increasing the particle density and magnetic field strength, and can thus make bright radio features. Shocks induced by interaction of a steady jet with fixed discontinuities in the surrounding medium (e.g., by the transition from a galactic atmosphere to a cluster atmosphere as discussed above) will be stationary. In completely symmetric outflows, such shocks will produce enhanced emission features ("knots" at low resolution) that are symmetrically placed about the nucleus. The brightness ratios between "corresponding" knots will be governed, through expression (1), by the *perturbed* jet velocity field $\mathbf{v}_j$ near the shocks. As there are more perturbations of the velocity field (both in v_j and in ι) that will decrease the Doppler boost of the flow than will increase it, the brightness ratios between knots are likely to be less than those between the preshock regions of the same flows. The brightest parts of the counterjets in relativistic flows containing stationary shocks are therefore most likely to be faint knots *at the same apparent distances from the core* as brighter knots in the main jets. This is also not what we have observed in 3C 219.

c) Symmetric Relativistic Flows with Moving Shocks

An apparent spatial asymmetry can be added to the above picture by light-travel time effects if the jets contain shock patterns that move at $\beta \approx 1$. Such moving shock patterns might be produced by time variations in the jet properties, or in the environment, or by interactions between the outward-moving jet and eddies in its own backflow (Smarr *et al.* 1984). The *observed* knot separations in the jet and counterjet could then be governed by the positions of the shocks at two different times in the development of the two jets, even if the shock structures are intrinsically symmetric around the core. If all shocks move outward, a given shock on the receding (counterjet) side is seen at an earlier proper time, and thus closer to the core, than its counterpart on the approaching (main jet) side. The ratio of the observed knot separations from the core in an intrinsically symmetric jet/counterjet system will then be

$$\left(\frac{1+\beta_s \sin \iota}{1-\beta_s \sin \iota}\right), \tag{2}$$

where $v_s = \beta_s c$ is the shock (pattern) velocity ($v_s < v_j$).

Relativistic flows containing intrinsically symmetric moving shocks might therefore be expected to contain inner (preshock) regions whose observed brightness ratios are governed by expression (1), then to develop *asymmetrically placed* knots whose observed separation ratios would be given by expression (2). As discussed above, the perturbation of the flow velocities near the shocks is likely to make the brightness ratio between the corresponding knots less than that in the preshock flow, except in a few "accidental" geometries in which passage through the shock pattern increases the Doppler factor of the approaching flow. The brightest parts of counterjets in this picture are therefore likely to be knots that appear to be *closer to the core* than their counterparts in the main jets. This picture matches, at least qualitatively, what we have seen in 3C 219, so we now explore it in more detail.

d) A Relativistic Jet Interpretation of 3C 219

In the symmetric moving-shock picture, the counterjet knot in 3C 219 could be the receding counterpart of the brightest knots in the main jet, their different apparent separations Θ_j and Θ_{cj} from the core resulting from the finite light-travel time across the source. The observed ratio $\Theta_j/\Theta_{cj} = 3.6$ (18″ to 5″) would require $\beta_s \sin \iota = 0.57$, where $v_s = \beta_s c$ is the shock velocity. This would require $\iota > 35°$, a statistically acceptable constraint. Comparison with the (axisymmetric) hydrodynamic beam cap simulations of Wilson and Scheuer (1983) and of Smith *et al.* (1985) shows that this inclination constraint is also consistent with the observation (Fig. 1 and PBWF) that 3C 219 has a V-shaped hot spot on the main-jet (approaching) side and a ring-like hot spot on the counterjet (receding) side of the source.

The observed brightness ratio $\mathcal{S}$ between the brightest jet knots and the counterjet knot is 11:1, whereas that between the inner parts of the jet and the counterjet is > 25:1 in some places. A benchmark for interpreting these ratios is given by expression (1) with $\beta_s \sin \iota = 0.57$, given that $\beta_j \geqslant \beta_s$. For $\alpha = 0.8$, $\mathcal{S}$ should be $\geqslant$36:1 in the inner parts of the jet—this is clearly consistent with our observations, but increased sensitivity and dynamic range are needed to test it directly.

Could the reduction of $\mathcal{S}$ from > 25:1 to 11:1 at the coun-

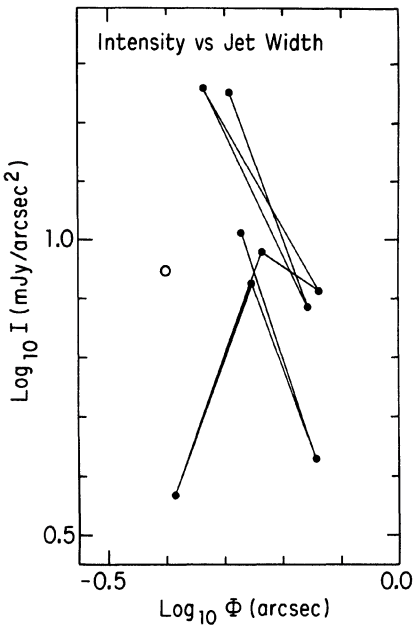

FIG. 7. Plot of the logarithm of the deconvolved peak intensity of the jet (normalized to millijanskys per square arcsecond) against the logarithm of the deconvolved transverse FWHM Φ (in arcseconds), at the locations where profiles were taken for Fig. 6 and for Table I. The connecting lines show the sequence of the points along the jet, demonstrating that for all but the datum from the weakest point in the jet, the slope of the $I - \Phi$ relationship is roughly constant. The datum for the counterjet knot is shown as the light circle; it also lies far from the mean $I - \Phi$ relationship exhibited by the main jet.

terjet knot instead be attributed to expansion from the observed width $\Phi = 0''.4$ in the counterjet knot to the observed $\Phi = 0''.5$ in the main-jet knot? This would require that the jet intensity vary from FWHM as $\Phi^{-5.3}$, close to the adiabatic brightness decline of $\Phi^{-5.67}$ for a constant-velocity circular jet with $\alpha = 0.8$ when the dominant magnetic field is parallel to the jet axis [e.g., Perley *et al.* 1984, Eq. (10)]. Expansion might be considered an alternative to velocity disordering as a means of reducing $\mathcal{S}$ if such an adiabat was followed. Figure 7 shows, however, that the main jet has a much less steep $I - \Phi$ law. Ignoring the $I - \Phi$ datum from the faint region of the jet $\sim 13''$ from the core (which appears uncorrelated with those in the brighter regions) the jet emission generally follows $I \propto \Phi^{-2.3 \pm 0.6}$, much slower than the adiabat required to explain the observed knot brightness ratio as an expansion effect. Disordering the velocity field therefore seems a more plausible explanation of the 11:1 ratio between the knot brightnesses, when the knots are interpreted using a moving-shock model. (The presence of the shocks may also, of course, explain the subadiabatic $I - \Phi$ variation).

A bend in the jets could also contribute to the decrease in $\mathcal{S}$ at the counterjet knot. A bend in the counterjet similar to the observed 11° "kink" in the main jet could make $\mathcal{S}$ larger near the core by increasing $\beta_j \sin \iota$ there.

Finally, we note that moving shocks may also arise if the jet entrains, or collides with, ambient clouds (e.g., Blandford and Königl 1979a,b; Henriksen 1984a). If this occurs, the shocks in the jet and counterjet could be intrinsically asymmetric around the core. If, moreover, a real collision occurs between the jet and a cloud (i.e., if the mean-free path in the cloud for a jet particle is less than the cloud scale), then initially a strong shock should appear. This could be a most effective means of decelerating a counterjet and of removing an unfavorable beaming from it. In time, however, this situation would translate itself into an accelerating terminal shock. If moving shocks are introduced into relativistic jets by such jet-cloud interactions, the asymmetries in the observed knot locations would be governed by randomness in the cloud geometry rather than by expression (2) above. As there is indeed evidence for such cloud-jet interactions in some radio galaxies (e.g., van Breugel *et al.* 1985), we emphasize that the above interpretations of knot asymmetries in terms of *symmetric* relativistic jets are not mandatory.

We conclude that a relativistic jet containing intrinsically symmetric fast-moving shocks could readily display apparent asymmetries similar to those we have observed in 3C 219. This interpretation cannot, however, be regarded as obligatory, as key details (jet orientation, shock speeds, and the jet-velocity field near the shocks) cannot be constrained either *ab initio* or by our data. Detection of the rest of the counterjet, and further exploration of its scale and brightness asymmetries relative to the main jet, would add important constraints to this discussion. In this context, it is interesting that (at least mildly) relativistic jet velocities are plausible in 3C 219 if the jet is assumed to supply energy steadily to the lobes (a) at a rate that balances the synchrotron luminosity of the lobes and (b) with enough thrust to overcome the minimum pressures in the lobe hot spots. Making this calculation as in Perley *et al.* [1984, Eq. (17)], we estimate $v_j \approx 0.038 c \xi^2 \epsilon^{-1}$, where ξ is the ratio of v_j in the frame of the hot spot to v_j in the frame of the galaxy, and ϵ is the efficiency with which energy conveyed into the lobe by the jet is converted into synchrotron radiation. For $\xi \approx 1$, $v_j \approx c$ is required to maintain this energy and thrust balance unless $\epsilon \gg 0.04$.

The Doppler boost implied by these relativistic jet models for the source asymmetries need not alleviate the jet-confinement problem. The crucial point is that the projection out of the plane of the sky that boosts the observed jet intensity in these models also increases—by a factor of sec ι—the scale size r_c that must be inferred for the confining gas (cf. Bridle 1986). As the predicted x-ray luminosity $L_x \propto r_c^3$, this increase in r_c offsets the reduction in p_j, unless the jet is near the orientation that maximizes its Doppler boost. Stated another way, in order to reduce the x-ray luminosity that is required for thermal confinement by invoking the Doppler boost, one must appeal to more extreme orientations of the jet than are needed to explain its asymmetries. To reduce L_x by a factor of 3 requires $\iota > 65°$, and to reduce it by a factor of 10 requires $\iota > 80°$, whereas $\iota > 35°$ is sufficient to explain the jet/counterjet asymmetries.

VIII. EPISODIC JET MODELS

To account fully for the appearance of the jet in 3C 219, we must also explain the failure of the main jet to reach the hot spot in the southern lobe. In this context, we think it significant that the brightness enhancements and the locally anomalous $\mathbf{B}_a$ configuration at the ends of both jets in 3C 219 resemble common properties of hot spots in radio lobes (e.g., Dreher 1980; Laing 1981a). Such hot spots are conventionally interpreted as strong slowly moving shocks near the *ter-*

minations of steady jets. However, to account for the lack of jet emission beyond the brightest jet knots in 3C 219 in a steady-jet picture would require either that the dissipation of the flow energy to synchrotron radiation drastically decreases beyond 35 kpc from the core, or that the jet flow becomes drastically decollimated at this distance and thus becomes "lost" against the lobe emission. The first assumption is distressingly *ad hoc*, while the second makes it difficult to account for the small sizes of the bright hot spots in both lobes of 3C 219.

It is therefore attractive to consider the possibility that the features at the ends of the jets in 3C 219 arise, by analogy with lobe hot spots, through compression of the lobeward ends of "young" jets that are re-establishing their channel through a resistive medium after a period of inactivity. Such jets should develop strong outward-moving shock structures near their tips; in this picture, the moving shocks invoked in Secs. VII*c* and VII*d* above would be both the first and last such shocks in the 3C 219 jets. This mechanism would require that shocks be present at the ends of both jets, leading naturally to the appearance observed in 3C 219 if the shock advance velocity is relativistic.

We emphasize, however, that the unsteady flow, or episodic behavior, required to explain the jet properties fully in this way could also be invoked directly to provide an alternate, but again *ad hoc*, rationalization of the other asymmetries in the source without appealing to $v_j \approx c$. In this sense, the postulate of an unsteady (episodic) flow is the most powerful part of such an interpretation.

If the counterjet knot is considered to be reflected through the core, it lies at the outer edge of the initial gap between the core and the main jet. In a relativistic jet interpretation of 3C 219, this would be written off as a mere geometrical coincidence. This placement of the counterjet emission, is, however, consistent with the *simplest* form of "flip-flop" episodic behavior (Rudnick and Edgar 1984), whereby energy transport occurs alternately (and at constant but not necessarily relativistic velocities) to the southwest and northeast of the core. In such a simple flip-flop interpretation, the absence of emission beyond the end of the main jet would imply that the energy flow on the southwest side of the source has been interrupted for $> 3.3h^{-1} \times 10^5$ yr. This is compatible with the symmetry of the 4885 MHz emission from the hot spots, as the synchrotron lifetimes of the electrons radiating at 4885 MHz in the equipartition fields of the hot spots would be much longer than this—$5h^{-3/7} \times 10^6$ yr. Thus, a flip-flop model could explain the known asymmetries of 3C 219 without conflict with its symmetries.

There may be little physical distinction between such episodic or flip-flop jets and the "independent plasmoids" of Christiansen *et al.* (1977). Adjustment of the ejection-velocity and ejection-interval parameters of such models may also provide *ad hoc* rationalizations for variation of FWHM Φ with angle Θ from the core. An unsatisfying (though not disqualifying) aspect of such interpretations is that, although they can *match* many aspects of the data, they cannot *predict* them—none of their important parameters can be constrained *ab initio*. They also do not explain why other radio galaxy jets (Sec. V) have similar $\Phi(\Theta)$ variations.

IX. CONCLUSIONS

Our new data confirm that the main jet in 3C 219 spreads much more slowly beyond $10h^{-1}$ kpc from the core than it does *on average* closer to the core. They also show that recollimation on the $\sim 10h^{-1}$ kpc scale by thermal pressure of a *galactic* atmosphere is not favored by the available x-ray data, but recollimation by a hotter *cluster* atmosphere cannot be ruled out and indeed appears plausible. Critical observations to test the jet collimation mechanism were discussed in Secs. V and VI.

It is possible to ascribe the major asymmetries of the jet and counterjet in 3C 219 to bulk relativistic motions in an intrinsically symmetric jet/counterjet system if the jet contains moving shocks. The observed variations in brightness ratio between the jet and the counterjet are more likely to arise from disordering of the velocity field at such moving shocks than from adiabatic expansion, because the intensity-width variation along the main jet appears to be significantly subadiabatic. To explain the abbreviated structure of this jet fully in a steady-jet model, its brightness variations must be ascribed to an arbitrary *potpourri* of shock formation, variable dissipation of the bulk energy in the flow to synchrotron radiation, and perhaps jet bending, as functions of distance from the core.

Alternatively, the lobeward brightening of the ends of both jets, the locally anomalous magnetic field configurations at these brightenings, and the anticorrelation between the separations of the jet knots from the core on the two sides, are simply compatible with an *unsteady* flow description wherein the nucleus of 3C 219 sporadically ejects material whose leading edge is compressed by ram pressure of the surrounding medium, leading to the observed brightenings and changes in $\mathbf{B}_a$ at these features. We emphasize that if the possibility of an unsteady flow is admitted, the arguments for relativistic outflow in this source cease to be compelling, and a simple, though also *ad hoc*, flip-flop interpretation also becomes admissible.

The jet/counterjet asymmetries might also be the result of strong shock formation in both jets by jet-cloud collisions at random distances from the core; in this case the appearance of the jets would be a manifestation of circumgalactic "weather" (Rees 1982) rather than of bulk relativistic motions.

Clearly, our new observations of 3C 219 leave many more questions unsettled than they answer. To fit the detailed structure of this source into any description of symmetric, steady energy transport in extragalactic sources requires the introduction of *ad hoc* complications. It may, however, be premature to conclude that we are involved with the "meteorology" featured by Rees, as 3C 219 appears to exhibit some properties of less conventional (episodic, or flip-flop) models.

We thank E. G. Ranch, H. Joseph, and L. Casita for stimulation and food for thought, and G. V. Bicknell, N. E. B. Killeen, and C. P. O' Dea for valuable comments on an earlier draft of this paper. We also thank S. F. Gull for many lively discussions about relativistic jets and their counterjets. R. N. H. acknowledges support by an operating grant from the Natural Sciences and Engineering Research Council of Canada (NSERC).

REFERENCES

Baars, J. W. M., Genzel, R., Pauliny-Toth, I. I. K., and Witzel, A. (1977). Astron. Astrophys. Suppl. **61**, 99.

Begelman, M. C., Blandford, R. D., and Rees, M. J. (1984). Rev. Mod. Phys. **56**, 255.

Benford, G. (1979). Mon. Not. R. Astron. Soc. **183**, 29.

Benford, G. (1983). In *Astrophysical Jets*, edited by A. Ferrari and A. G. Pacholczyk (Reidel, Dordrecht), p. 271.

Bicknell, G. V. (1986). Astrophys. J. **300**, 591.

Bicknell, G. V., and Henriksen, R. N. (1980). Astrophys. Lett. **21**, 29.

Blandford, R. D., and Königl, A. (1979a). Astrophys. J. **232**, 34.

Blandford, R. D., and Königl, A. (1979b). Astrophys. Lett. **20**, 15.

Bradshaw, P. (1981). In *AFOSR-HTTM Stanford Conference on Complex Turbulent Flows*, edited by S. J. Klein, B. J. Cantwell, and G. H. Lilley (Stanford University, Stanford, CA), p. 364.

Bridle, A. H. (1982). In *Extragalactic Radio Sources*, IAU Symposium No. 97, edited by D. S. Heeschen and C. M. Wade (Reidel, Dordrecht), p. 121.

Bridle, A. H. (1984). Astron. J. **89**, 979.

Bridle, A. H. (1986). Can. J. Phys. **64**, 353.

Bridle, A. H., Chan, K. L., and Henriksen, R. N. (1981). J. R. Astron. Soc. Can. **75**, 69.

Bridle, A. H., Henriksen, R. N., Chan, K. L., Fomalont, E. B., Willis, A. G., and Perley, R. A. (1980). Astrophys. J. Lett. **241**, L145.

Bridle, A. H., and Perley, R. A. (1984). Annu. Rev. Astron. Astrophys. **22**, 319.

Burch, S. F. (1979). Mon. Not. R. Astron. Soc. **186**, 519.

Cavaliere, A., and Fusco-Femiano, R. (1976). Astron. Astrophys. **49**, 137.

Chan, K. L., and Henriksen, R. N. (1980). Astrophys. J. **241**, 534.

Christiansen, W. A., Pacholczyk, A. G., and Scott, J. S. (1977). Nature **266**, 593.

De Young, D. S., Hogg, D. E., and Wilkes, C. T. (1979). Astrophys. J. **228**, 43.

Dreher, J. W. (1981). Astron. J. **86**, 833.

Fabbiano, G., Miller, L., Trinchieri, G., Longair, M., and Elvis, M. (1984). Astrophys. J. **277**, 115.

Fabricant, D., Lecar, M., and Gorenstein, P. (1980). Astrophys. J. **241**, 552.

Fanaroff, B. L., and Riley, J. M. (1974). Mon. Not. R. Astron. Soc. **167**, 31P (FR).

Fanti, R., Lari, C., Parma, P., Bridle, A. H., Ekers, R. D., and Fomalont, E. B. (1982). Astron. Astrophys. **110**, 169.

Forman, W., Jones, C., and Tucker, W. (1985). Astrophys. J. **293**, 102.

Henriksen, M. J., and Mushotzky, R. F. (1983). Astrophys. J. **292**, 441.

Henriksen, R. N. (1984a). In *Physics of Energy Transport in Extragalactic Radio Sources*, Proceedings of NRAO Workshop No. 9, edited by A. H. Bridle and J. A. Eilek (NRAO, Green Bank, WV), p. 122.

Henriksen, R. N. (1984b). In *Physics of Energy Transport in Extragalactic Radio Sources*, Proceedings of NRAO Workshop No. 9, edited by A. H. Bridle and J. A. Eilek (NRAO, Green Band, WV), p. 211.

Högbom, J. A. (1979). Astron. Astrophys. Suppl. **36**, 173.

Jones, C., and Forman, W. (1984). Astrophys. J. **276**, 38.

Killeen, N. E. B., Bicknell, G. V., and Ekers, R. D. (1986). Astrophys. J. **302**, 306.

Königl, A., and Choudhuri, A. R. (1985). Astrophys. J. **289**, 173 (KC).

Laing, R. A. (1981a). Mon. Not. R. Astron. Soc. **195**, 261.

Laing, R. A. (1981b). Astrophys. J. **248**, 87.

Lau, J. C. (1981). J. Fluid. Mech. **105**, 193.

Lea, S. M., Mushotzky, R., and Holt, S. S. (1982). Astrophys. J. **262**, 24.

Ledden, J. E., Broderick, J. J., Condon, J. J., and Brown, R. L. (1980). Astron. J. **85**, 780.

Matthews, T. A., Morgan, W. W., and Schmidt, M. (1964). Astrophys. J. **140**, 35.

Miller, L. (1986). R. Obs. Edinburgh Prepr.

Mushotzky, R. (1985). In *Nonthermal and very High Temperature Phenomena in X-ray Astronomy*, edited by G. C. Perola and M. Salvati (Istituto Astronomico, Universita "La Sapieaza," Rome), p. 105.

Perley, R. A., Bridle, A. H., and Willis, A. G. (1984). Astrophys. J. Suppl. **54**, 291.

Perley, R. A., Bridle, A. H., Willis, A. G., and Fomalont, E. B. (1980). Astron. J. **85**, 499 (PBWF).

Rees, M. J. (1982). In *Extragalactic Radio Sources*, IAU Symposium No. 97, edited by D. S. Heeschen and C. M. Wade (Reidel, Dordrecht), p. 211.

Rudnick, L., and Edgar, B. K. E. (1984). Astrophys. J. **279**, 74.

Sanders, R. H. (1983). Astrophys. J. **266**, 73.

Schmidt, M. (1965). Astrophys. J. **141**, 1.

Simard-Normandin, M., Kronberg, P. P., and Button, S. (1981). Astrophys. J. Suppl. **45**, 97.

Smarr, L. L., Norman, M. L., and Winkler, K. H.-A. (1984). Physica **12D**, 83.

Smith, M. D., Norman, M. L., Winkler, K.-H. A., and Smarr, L. L. (1985). Mon. Not. R. Astron. Soc. **214**, 67.

Thompson, A. R., Clark, B. G., Wade, C. M., and Napier, P. J. (1980). Astrophys. J. Suppl. **44**, 151.

Turland, B. D. (1975). Mon. Not. R. Astron. Soc. **172**, 181.

van Breugel, W., Miley, G., Heckman, T., Butcher, H., and Bridle, A. (1985). Astrophys. J. **290**, 496.

Willis, A. G., Strom, R. G., Bridle, A. H., and Fomalont, E. B. (1981). Astron. Astrophys. **95**, 250.

Wilson, M. J., and Scheuer, P. A. G. (1983). Mon. Not. R. Astron. Soc. **205**, 449.